PAPER • OPEN ACCESS

Investigation on Microstructure and Mechanical Properties of ATIG welded alloy C-276 with Fe$_2$O$_3$ flux

View the article online for updates and enhancements.

IOP ebooks™

Bringing you innovative digital publishing with leading voices to create your essential collection of books in STEM research.

Start exploring the collection - download the first chapter of every title for free.

Investigation on Microstructure and Mechanical Properties of ATIG welded alloy C-276 with Fe₂O₃ flux

Angad Surve[1], Sharnappa Bhosage[1], Akshay Mehta[1], Srikanth A[1], Arivarasu M[2], Manikandan M[1], *Gokulkumar K[1], Deva.N.Rajan[3]
[1]School of Mechanical Engineering, VIT University, Vellore, India
[2]Centre for Innovative Manufacturing Research, VIT University Vellore India
[3]Delta Weartech Engineers, Chennai, India

*E-mail: gokulkumar510@gmail.com

Abstract. Alloy C-276 susceptible to hot cracking. The microsegregation occurs during solidification is the largely responsible for the hot cracking in the alloy. The present study investigates the microstructure and mechanical properties of alloy C-276 weld joint fabricated by ATIG welding technique. The macro examination was carried out assess the defects in the weld joints. Optical and scanning electron microscope examination was carried out to see the structural changes in the fusion zone. The tensile test was performed to evaluate the strength of the weld joints. The results show the defect free welding was achieved in the established process parameters. The macrograph shows the full depth of penetration was obtained in the single pass by the effect of Marangoni convection. Energy Dispersive X-ray spectroscopy (EDS) analysis illustrates the absence of microsegregation in the interdendritic zone. The tensile test shows the improved mechanical properties compared to the base metal.

Keyword: Alloy C-276, Microsegregation, Activated Tungsten Inert Gas Welding.

1. Introduction

Alloy C-276 is a Nickel based superalloy derived from Ni-Cr-Mo ternary system [1]. The presence of Cr and Mo provides the excellent corrosion resistance in oxidizing and reducing environments [2]. Alloy C-276 has been a wide range of applications in marine environments. Alloy C-276 is a workhorse material for the construction of flue gas desulfurization (FGD) in the power plant environment. Welding of alloy C-276 is possible by arc welding techniques like gas tungsten arc welding (GTAW) and gas metal arc welding (GMAW) [3]. The major problem associated with this alloy is the formation of secondary phases P and µ at the end of the solidification [4]. The formation of secondary phases is mainly due to the higher heat input during the multipass welding process. Cieslak et al. [4] reported that alloy C-276 prone to hot cracking due to the formation of topologically close-packed (TCP) phases such as P and µ. The authors observed these phases are mainly due to the segregation of alloying elements Mo and W at the end of the solidification. Manikandan et al. [2, 5-7] investigated the welding of alloy C-276 by GTA and PCGTA welding by using different filler wires (ERNiCrMo-3, ERNiCrMo-4, and ER2553) and autogenous mode. The authors reported that PCGTA welding shows reduced microsegregation compared to GTAW welding. The authors concluded that the faster solidification with lower heat input in the PCGTAW shows reduced microsegregation compared to GTAW. Also, the author highlights the improper selection of filler wires leads to higher segregation in the fusion zone. Few literatures reported that high-density welding process such as

electron beam welding and laser beam welding provides the good metallurgical and mechanical properties compared to the conventional welding process [8-10]. The authors reported that the faster solidification achieved in the high-density welding process avoids the formation of secondary phases during solidification.

In general, GTAW and GMAW are the most economical welding process in the industry environment. The major limitation in the GTAW is the limited thickness of the base metal can be welded in a single pass. Multipass Welding can be helped to achieve the high thickness, but higher heat input employed in the multipass welding leads to undesirable properties.

In the year 1950s, a novel technique was proposed by E.O. Paton Electric Welding Institute (Ukraine) to achieve the high depth of penetration in the conventional TIG welding by using organic compounds [11]. Fluid flow plays a major role in controlling the shape of the fusion zone in the TIG welding. Fluid flow in the molten zone is driven by surface tension, the Lorentz force, buoyancy and aerodynamic drag [12]. Many studies reported that the geometry of the fusion zone might vary by changing the concentration of one or more impurities in the base metal. Surface tension in the weld pool controls the fluid flow in the fusion zone. The surface active elements are very sensitive to alter the surface tension gradient. The surface active elements segregate the surface of the molten zone and modify the temperature in the fusion zone depends upon the surface temperature [13-15]. In general, the surface tension of metal and alloys normally decreases as temperature increases; that is the pure metal always negative surface tension gradient ($d\gamma/dT < 0$). The surface tension of the material will be high at the edge and low at the center of the weld pool. The surface tension gradient will tend to produce outward fluid flow. The weld geometry obtained the shallow weld. In order to get the higher depth of penetration, the surface active elements like oxygen and sulfur produce the positive surface tension gradient ($d\gamma/dT > 0$) in the molten pool. In this case, the surface tension will be high at the center and low at the edge of the weldment. The inward fluid flow obtained in the positive surface tension produced deep penetration [16-20].

Many literatures reported that ATIG welding produced more depth of penetration compared to conventional TIG welding process. The aim of the present study is to study the effect of ATIG welding on alloy C-276 by applying Fe2O3 flux on the surface of the molten pool. There is no study reported on alloy C-276 with reference to ATIG welding. There is a lot of scopes to study the welding of alloy C-276 by changing various surface active elements. In this present study, the authors choose Fe_2O_3 as the surface active elements. The microsegregation of alloying elements also examined in detail.

2. Material and Methodology

Nickel based superalloy C-276 was procured in the form of 4 mm thick plate in the hot rolled solution annealed condition. The chemical composition of the base metal is listed in table 1. The weld plate was cut in the dimensions of 55 X 130 X 4 mm by using wire cut electrical discharge machine (EDM).

Table 1. Chemical composition of as received alloy C-276

Base Metal	Chemical Composition (% Wt.)								
	Ni	Mo	Cr	W	Co	Mn	Fe	V	Others
Alloy C-276	Bal	16.36	15.83	3.45	0.05	0.41	6.06	0.17	0.005(P), 0.002 (S), 0.02 (Si), 0.005(C)

The plate was cut cleaned with acetone to remove the dirt. KEMPII DWE machine was employed to join the plate. The process parameters were established based on the bead on the plate. The finalized process parameters were listed in Table 2.

Table 2. Process Parameter of ATIG welded alloy C-276

Current (A)	120
Voltage	12

Argon was used as a shielding gas with a flow rate of 15 L/min. The Fe2O3 flux powder was employed in the present study to convert the negative surface tension into positive surface tension. The Fe_2O_3 power was mixed with methanol to obtain a paint link consistency and was applied over the surface of the joint manually using paint brush. The photograph figure 1 shows the weld plate photograph of ATIG welded alloy C-276 with Fe2O3 flux.
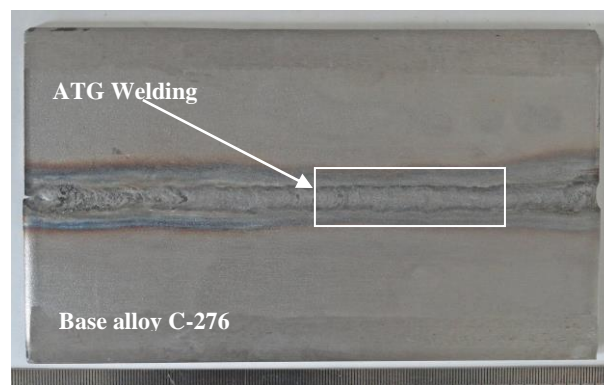

Figure 1 Photograph of Alloy C-276 ATIG
Weldment

Radiography examination was carried out to evaluate the defect in the weld joint. Macro and microstructure examination was conducted on the composite regions which consist of base metal, HAZ and weld zone. The samples were polished with 220 to 2000 gird SiC paper followed by 0.5 μ alumina powder and water polish to obtain the mirror finish. The microstructure was revealed with the mixed acids of 80 ml HCL, 4 ml HNO3, 20 ml glycerol and 1 g CuCl2 were used as an etchant. SEM /EDS analysis was carried out to evaluate the microsegregation of alloying elements in the fusion zone. The tensile test was carried out to assess the strength and ductility of the weld joints. Test specimens were prepared and confirmed to ASTM E8 standards. Tensile test was done in triplicate to ensure the repeatability of the results. The test was carried out in the ambient temperature. SEM fractography analysis was conducted to evaluate the mode of tensile failure specimen.

3. Results and Discussions

3.1. Weldment Quality

Radiography and macro examination were performed to assess the defects in the weld joints. The macro examination was carried out in three different regions in the fusion zone. The specimens were extracted in the both end and middle of the fusion zone. In general, the end portion has the maximum possibilities of defects such as porosity, cracks and lack of side wall [21]
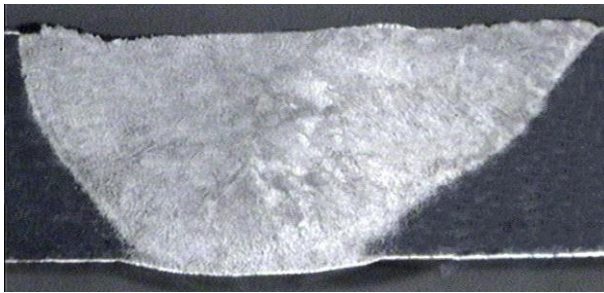
Figure 2 Macrostructure of the ATIG welded alloy
C-276

Figure 2 represents the macrograph of ATIG welding of alloy C-276 with Fe_2O_3 flux. The macrograph clearly shows that defect free welding was achieved in the process parameters employed in the present study. Also, it is observed that full depth of penetration was achieved in the single pass. The early studies reported by the same authors, in the conventional TIG welding the full penetration was achieved in two passes with higher current [2]. In the present study, the depth of penetration was achieved in the single pass. The macrograph shows the steady fluid flow in the weld pool and good welding morphology. The presence of Iron oxide converts the negative surface tension to the positive surface tension. The fluid flow in the molten zone is directed inward along the surface of the molten pool and downward towards the bottom. This leads to increase the depth of penetration of the weldment which is also known as the Marangoni convection [15-19].
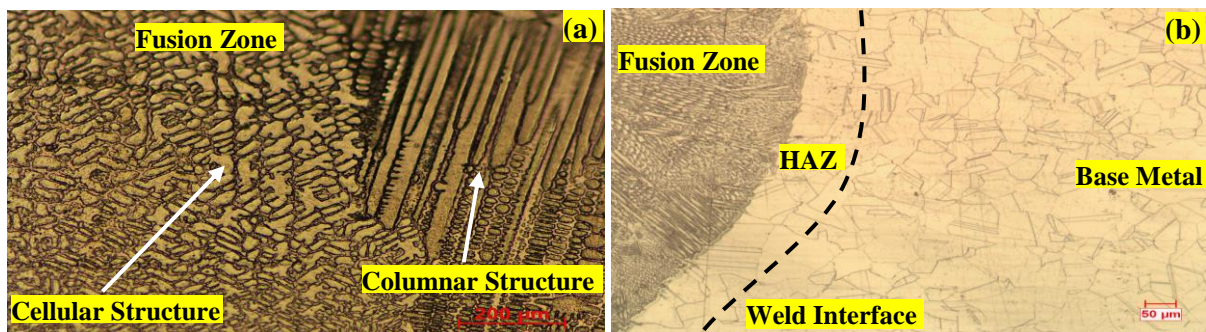
3.2 Microstructure Examination

Figure 3 Microstructure of ATIG welded alloy C-276 alloy a) Fusion Zone; b) Weld Interface

Figure 3 a-b represents the optical microstructure of base metal, weld interface and fusion zone of ATIG welded alloy C-276. The base metal microstructure consists of austenitic grain structure with annealing twins were observed in many of the grain boundaries. The microstructure of the fusion zone consists of cellular structures along with columnar dendrites. The weld interface regions show the planar and columnar dendrites. The variation of structure changes is due to thermal gradient [22]. The thermal gradient in a weld zone steeper close to fusion boundary than weld interior. The steep thermal gradients prevailing at the fusion boundary more favour to columnar dendrite growth in the direction opposite to the heat extraction. The presence of 58% of Ni in base metal shows the microstructure as austenitic structure. The grain boundaries are also well defined. Annealing twins are observed in many grain boundaries. The material was rolled at 1200 ℃ the twin boundaries are seen. The HAZ regions are clearly distinct in the dotted lines. As compared to conventional TIG welding the size of the HAZ regions is less in the ATIG welding. The lower heat input employed in the ATIG welding is largely responsible for the lesser HAZ. Coarser grains are not seen in the HAZ region.

3.3 SEM/EDS analysis

SEM/EDS micrograph of ATIG welded alloy C-276 is shown in Fig. 4. The higher magnification SEM micrograph (Fig. 4 (a & b)) shows the cellular and columnar dendrites in the fusion zone center and interface regions. EDS analysis was carried out to evaluate the microsegregation of alloying elements in the fusion zone. Emphasis was given to Ni, Cr, Mo, W and Fe. These alloying elements tend to form P and μ phases during solidification in the alloy C-276. Figure 4(i-ii) represents the EDS analysis of weld center dendrite core and interdendritic regions. Figure 4(iii-iv) accounts for the corresponding regions in the weld interface regions. In both regions, it is observed that the segregation is not observed. The chemical composition seen in the dendritic core and interdendritic regions are almost matching with the base metal chemical composition. The authors believed that the lower current (heat input) employed in the ATIG welding reduced the effect of microsegregation in the present study. The same authors reported that the alloy C-276 prone to hot cracking in the arc welding process. The authors indicated that the alloy fabricated by continuous current TIG welding shows higher segregation [2], whereas in the present research work the extent of segregation is suppressed. The present research work brings out the extent of microsegregation can be avoided by reduced heat input by adopting ATIG welding process.
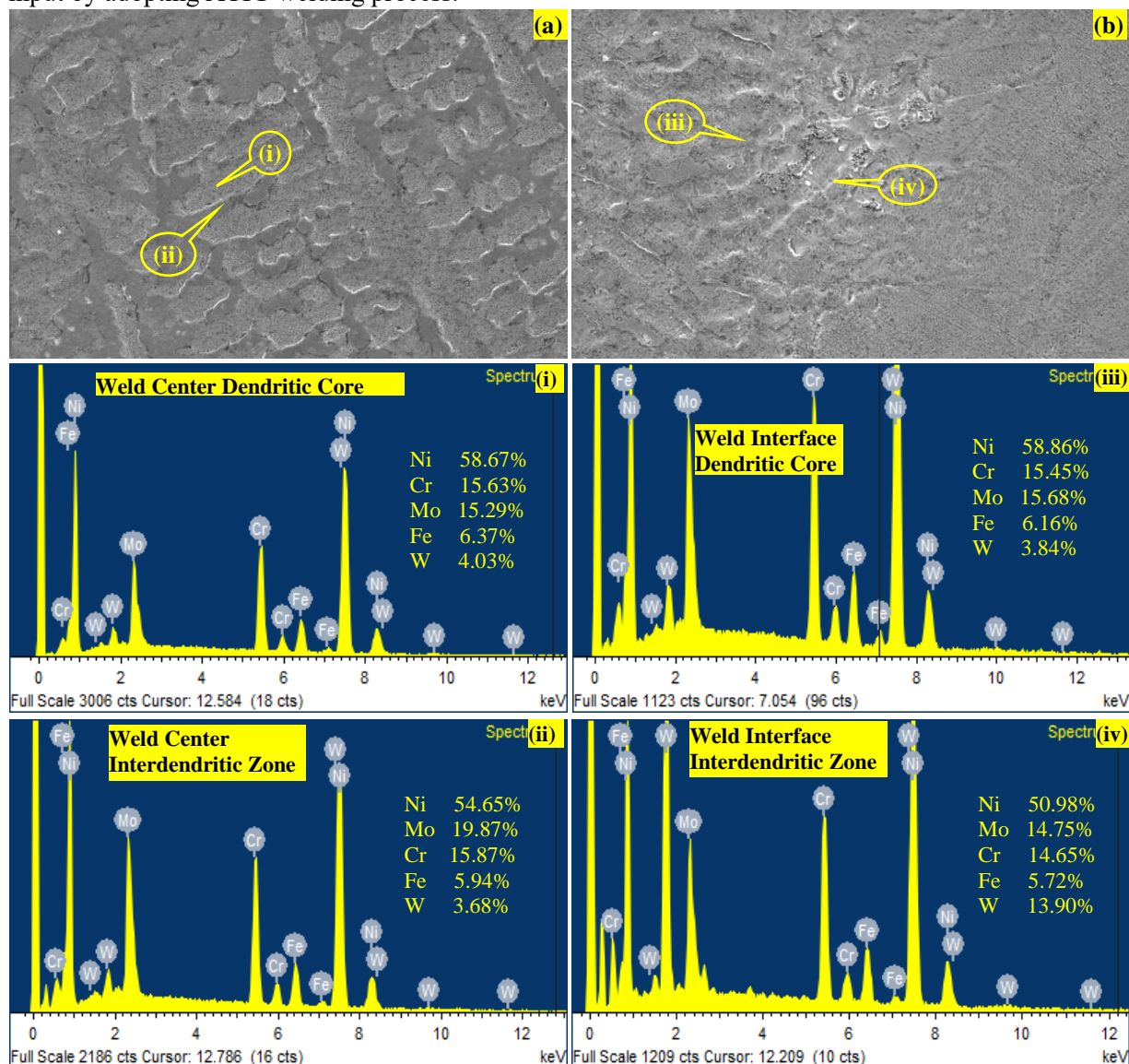

Figure 4 SEM/EDAX analysis of ATIG welded C-276 alloy for different places of weldment a) SEM-Weld Center; b) SEM-Weld Interface; i)Weld Center- Dendritic Core; ii) Weld Center- Interdendritic Zone; iii)Weld Interface- Dendritic Core; iv) Weld Interface- Interdendritic Zone

3.4 Mechanical Properties
3.4.1 Tensile test
The tensile test was carried out to evaluate the strength of the weld joints. Figure 5 shows the tensile failure samples. It is observed from the photograph that the fracture occurred in the fusion zone. The test was carried out triplicate to ensure the repeatability of the results. The average strength observed in the weldment zone was 780 MPa. Base metal strength also evaluated for the comparison purpose. The observed base metal strength was 750 MPa. The results show that the weldment is stronger than the base metal. SEM fractography (Fig. 6) analysis was carried out to evaluate the mode of fracture in the tensile failure sample. The results showed the presence of microvoid with elongated dimples and confirmed to the ductile mode of fracture. In general, the ductility is taken in account when the homogenous material is tested. In the weld joints three different regimes – Base metal, HAZ and fusion zone across the transverse cross section. Contribution is there from each region. The ductility cannot be treated as quantitative. In order to evaluate the ductility special experimental approach and more specific studies to be taken up in near future
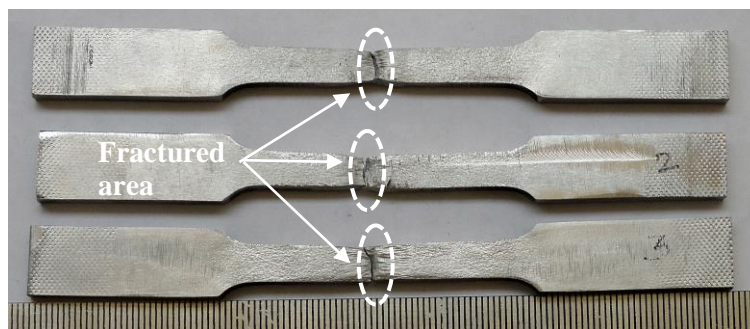

Figure 5 Photograph of failure tensile tested specimens of ATIG
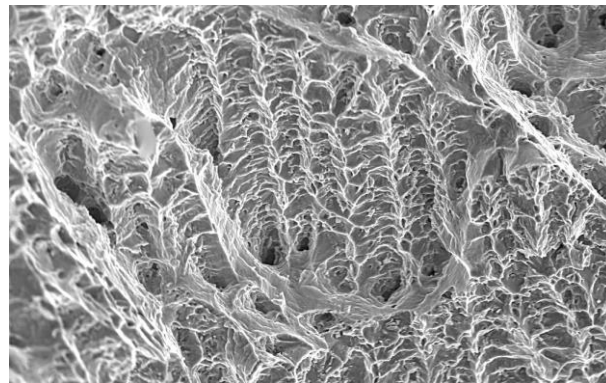welded C-276 alloy

Figure 6 SEM fractograph of tensile tested specimen

4. Conclusions

The major results obtained from the present study is listed.
1. Defect free weld joint was achieved in the established process parameters
2. The full depth of penetration was achieved in the single pass with the help of Fe_2O_3 flux.
3. Fe_2O_3 convert the negative surface tension to positive surface tension to achieve the full depth of penetration in the single pass
4. Columnar and cellular structure was observed in the fusion zones
5. The lower heat input reduced the effect of microsegregation in the fusion zone.

References

[1] Cieslak M J, Knorovsky G A, Headley T J and Romig A D 1986 *Jr. Metall.Trans* **17A** 2107–2116

[2] Manikandan M, Arivazhagan N, Nageswara Rao M and Reddy G M 2014 *J. Manuf. Processes* **16** 563-572

[3] http://www.specialmetals.com/documents/Inconel%20alloy%20C-276.pdf. 2011

[4] Cieslak M J, Headley T J and Romig A D 1986 *Jr. Met. Trans A* **17A** 2035-2047

[5] Manikandan M, Arivazhagan N, Rao M N and Reddy G M 2015 *Acta Metall. Sin.* **28** 208–215

[6] Manikandan M, Arivazhagan N, Arivarasu M, Mageshkumar K, Rajan Deva N, Arul Murugan B, Prasanth P, Sukumar S and Vimalanathan R 2017 *Trans Indian Inst Met* **70(3)** 661-669

[7] Savyasachi Pandit, Vaibhav Joshi, Meghna Agrawal, Manikandan M, Devendranath Ramkumar K, Arivazhagan N and Narayanan S 2014 *Procedia Eng.* **75** 61-65

[8] Manikandan M, Hari P R, Vishnu G, Arivarasu M, Devendranath Ramkumar K, Arivazhagan N and Reddy G M 2014 *Procedia Mater. Sci*. 2233-2241

[9] Guangyi M A, Dongjiang W U and Dongming G U O 2011 *Metall. Mater. Trans. A* **A42** 3853–3857

[10] Hashim M, SarathRaghavendraBabu K E, Duraiselvam M and Natu H 2013 *Mater. Des.* **46** 546-551

[11] Gurevich S M, Zamkov V N and Kushnirenko N A 1965 *Avtom. Svarka.* **18** 1–4

[12] Kuang-Hung Tseng and Ko-Jui 2012 *Powder Technol.* **228** 36–46

[13] Heiple C R, Cluley R J and Dixon R D 1980 *Physical metallurgy of metal joining*160-165.

[14] Savage W F, Nippes E F and Goodwin G M 1977 *Weld. J.* **56(4)** 126s-132s

[15] Heiple C R and Roper J R 1982 *Weld. J.* **61(4)** 97s-102s

[16] Heiple C R and Roper J R 1981 *Weld. J.* **60(8)** 143s–145s

[17] Roy C, Pavanan V.V, Vishnu G, Hari P.R, Arivarasu M, Manikandan, M, Ramkumar D. Arivazhagan N , 2014. Procedia Mater. Sci., **5** 2503-2512.

[18] Heiple C R, Roper J R, Stagner R T, Aden R J 1983 *Weld. J.* **62(3)** 72–77

[19] Heiple C R, Burgardt P 1985 *Weld. J.* **64(6)** 159–162

[20] Burgardt P, Heiple C R 1986 *Weld. J.* **65(6)** 150–155

[21] Pavan A H V, Vikrant K S N, Ravibharath R, Kulvir Singh 2016 *Mater. Sci. Eng., A* **651** 32 - 41

[22] Janakiram G D, Venugopal Reddy A, Prasad Rao K, Madhusudhan Reddy G 2004 *J. Sci. Technol. Weld. Join.* **9(5)** 390–398